



Active fault system across the oceanic lithosphere of the Mozambique Channel: Implications for the Nubia–Somalia southern plate boundary

Eric Deville, Tania Marsset, Simon Courgeon, Romain Jatiault, Jean-Pierre Ponte, Estelle Thereau, Gwenael Jouet, Stéphan Jorry, L. Droz

► To cite this version:

Eric Deville, Tania Marsset, Simon Courgeon, Romain Jatiault, Jean-Pierre Ponte, et al.. Active fault system across the oceanic lithosphere of the Mozambique Channel: Implications for the Nubia–Somalia southern plate boundary. *Earth and Planetary Science Letters*, 2018, 502, pp.210-220. 10.1016/j.epsl.2018.08.052 . hal-01901914

HAL Id: hal-01901914

<https://hal.univ-brest.fr/hal-01901914>

Submitted on 10 Dec 2018

HAL is a multi-disciplinary open access archive for the deposit and dissemination of scientific research documents, whether they are published or not. The documents may come from teaching and research institutions in France or abroad, or from public or private research centers.

L'archive ouverte pluridisciplinaire **HAL**, est destinée au dépôt et à la diffusion de documents scientifiques de niveau recherche, publiés ou non, émanant des établissements d'enseignement et de recherche français ou étrangers, des laboratoires publics ou privés.

1 **Active fault system across the oceanic lithosphere of the Mozambique Channel:**
2 **Implications for the Nubia-Somalia southern plate boundary**

3

4 Eric Deville^{a*}, Tania Marsset^b, Simon Courgeon^{b,c}, Romain Jatiault^{d,e}, Jean-Pierre Ponte^f,
5 Estelle Thereau^b, Gwenael Jouet^b, Stéphan J. Jorry^b, Laurence Droz^g

6

7 ^a*IFPEN-IFP School, 1-4 avenue de Bois-Préau, 92852 Rueil-Malmaison, France*

8 ^b*IFREMER, Unité Géosciences Marines, 29280 Plouzané, France*

9 ^c*University of Geneva, Département of Earth Sciences, Rue des Maraichers 13, CH-1205 Geneva, Switzerland*

10 ^d*TOTAL, Exploration and Production, CSTJF, Avenue Larribau, 64000 Pau, France*

11 ^e*CNRS, Laboratoire CEFREM, Avenue Paul Alduy, 66000 Perpignan, France*

12 ^f*Université de Rennes 1, campus Beaulieu OSUR, 35042 Rennes cedex, France*

13 *Université de Bretagne occidentale, IUEM, 29280 Plouzané, France*

14

15 **ABSTRACT**

16

17 Seismic reflection and multibeam echosounder data were acquired in the Mozambique Channel in
18 2014 and 2015 during the PTOLEMEE, PAMELA-MOZ02 and -MOZ04 marine surveys aboard the
19 *RV Atalante* and *Pourquoi Pas?* These data revealed that an active fault system is deforming the
20 oceanic lithosphere of the Mozambique Basin which has developed during Jurassic-Cretaceous times.
21 The correlation between the fault system and the arrangement of earthquake epicenters suggests that
22 this tectonically active zone directly connects northward with the southern part of the eastern branch of
23 the East African Rift System which corresponds to the seismically active graben system bounding the
24 northern part of the Davie ridge. The fault zone extends southwestward of the Mozambique Ridge
25 along the same trend as the Agulhas-Falkland transform fault zone. The general organization of the
26 fault zone shows the characteristics of an extensional system north of the Mozambique Channel (north
27 of the Europa Island) and a right-lateral transtensional system with coeval normal faults and strike-slip

28 faults south-west of Europa. This tectonic activity is associated with volcanic activity since at least
29 Late Miocene times. Our findings emphasize that the eastern branch of East African Rift System is
30 extending largely toward the south, not only in continental domains but also through the oceanic
31 lithosphere of the Mozambique basin. This fault zone is participating to the complex plate boundary
32 between the main African continent (Nubia Plate) and Madagascar (Somalia Plate).

33

34 *Keywords:* Active faults, Mozambique Channel, plate boundary, Nubia plate, Somalia plate

35

36 * Corresponding author

37

38 **1. Introduction**

39

40 The East African Rift System (EARS), originally described by Suess (1891), corresponds
41 to the northern part of the divergent plate boundary system between the Nubian (West
42 African) and Somali (East African) plates. This rift system is connected northward to the Afar
43 hot spot which is related to the opening of the Red Sea and the Gulf of Aden, which began
44 being active about 30 Ma ago. However, it is considered that the EARS began to be active
45 only later, starting 24 Ma ago in the Afar area (Chorowicz, 2005). Although the EARS is
46 commonly considered as the modern archetype of rifted plate boundaries, the current Nubia-
47 Somalia kinematics is among the least well-known of all the major plate boundaries (Calais et
48 al., 2006; Stamps et al., 2008). The plate boundary between Nubia and Somalia developed
49 over thousands of kilometers across the eastern part of Africa during Late Oligocene and
50 Neogene times (Chorowicz, 2005; Ebinger, 2012; McGregor, 2015). The location of the plate
51 boundaries is well-defined along the continental branches of the EARS which include a
52 western branch and an eastern branch (Fig. 1). The eastern branch (Gregory Rift) is
53 characterized by high volcanic activity (including Mount Kilimanjaro, the highest point of
54 Africa) and the western branch (Albertine Rift) is characterized by a moderate volcanic
55 activity relative to the eastern branch and by deeper basins, containing lakes and sediments.
56 The Great Lakes (Albert, Tanganyika, Rukwa, Malawi) are located in highly rifted basins
57 bounded by normal and strike-slip faults of the western branch of the EARS. The two
58 branches of the EARS delineate major relatively poorly deformed blocks: Victoria and
59 Rovuma (Hartnady, 2002; Calais et al., 2006; Stamps et al., 2008, 2014; Fernandes et al.,
60 2013; Saria et al., 2014; Fig. 1). The eastern branch of the EARS extends off Tanzania and in
61 the northern part of the Mozambique offshore, bounding notably the Davie Ridge (Mougenot

et al., 2005; Mahanjane et al., 2014 a & b; Franke et al., 2015; Mulibo and Nyblade, 2015). But south of the Davie Ridge in the eastern branch and south of the Machaze epicentral area in the western branch (Fig. 1 & 2), the exact location of the EARS still remains a topic of discussion. Scattered extensional structures associated with seismic activity are found onshore in Mozambique, Swaziland and South Africa (Foster and Jackson, 1998; Yang and Chen, 2010; Fonseca et al., 2014; Domingues et al., 2016) and also along the Comores and Mayotte islands and within Madagascar (Grinison and Chen, 1988; Bertil and Regnoult, 1998; Kusky et al., 2007, 2010; Michon, 2016; Fig. 1). Active tectonics across Madagascar has been interpreted as a possible extension connected to the East African Rift System (Kusky et al., 2007; 2010). It forms a segment running through Comores, across Madagascar and finally extends to the Southwest Indian spreading ridge. This extension is associated to Neogene-Quaternary alkaline volcanic activity associated with active hot springs. It also causes high and young topography and seismic activity and it is probably associated to mantle rise under Madagascar (Kusky et al., 2010). Earthquakes have also been recorded within the Mozambique Channel (Hartnady, 2002; Stamp et al., 2008) but prior to this study no data were available to characterize structural evidence for recent to active deformation within the Mozambique Channel (Fig. 1). Marine geophysical surveys carried out in 2014 and 2015 provided evidence for a recent/active fault system running crossing the Mozambique Basin (Fig. 4). This paper aims providing an analysis of the spatial distribution of active faults as well as faults sealed by recent sediments within this area. We notably present some examples of bathymetric data and seismic lines showing these structures and we discuss the significance of this fault system in the plate tectonics framework of the East African offshore.

84

85 2. Geodynamic and geological framework

86

87 North of the Mozambique Channel, the southern extension of the eastern branch of the
88 EARS off Tanzania and Mozambique (eastern boundary of the Rovuma block) has been well-
89 established by seismic reflection data (Mougenot et al., 1986; Mahanjane, 2014a; Franke et
90 al., 2015), earthquake slip vector data and GPS data (Calais et al., 2006; Stamps et al., 2008;
91 Saria et al., 2014), and spatial distribution of earthquake focal mechanisms (Grimison and
92 Chen, 1988; Yang and Chen, 2010; Delvaux and Barth, 2010; Franke et al., 2015). The
93 offshore segment of the eastern branch of the EARS is characterized from north to south by
94 Neogene extension tectonics overimposed on former strike-slip structures of the Tanzanian-
95 northern Mozambique transform margin which have developed during Mid Jurassic-
96 Cretaceous times in relation with the drift of Madagascar with respect to Africa (Rabinowitz
97 et al., 1983; Coffin and Rabinowitz, 1987; Storey et al., 1995; Reeves, 2014; Franke et al.,
98 2015). Regarding the current kinematics of the plate boundary between Nubia and Somalia,
99 Chu and Gordon (1999) analysis placed the pole of rotation of Nubia versus Somalia in the
100 offshore of southeastern cost of South African, in the Mozambique Ridge or south of the
101 Mozambique basin (Fig. 1), which imply that south of the rotation pole, the southern part of
102 the Nubian-Somali plate boundary is a diffuse zone of convergence (up to $\sim 2\text{mm yr}^{-1}$). This
103 interpretation is consistent with subsequent work integrating seismicity studies (Horner-
104 Johnson et al., 2007) and coupled seismicity-GPS studies (Calais et al., 2006; Stamps et al.,
105 2008; Argus et al., 2010; DeMets et al., 2010; Saria et al., 2014; Stamps et al., 2014; Fig. 1).
106 Clusters of earthquake epicenters are located in continental Africa (Fonseca et al., 2014). In
107 addition, evidence for volcanism and tectonic activity characterized by earthquakes has been
108 reported along faults in the Comoros and Mayotte (Emerick and Duncan, 1982; Michon,
109 2016) and Madagascar (Kusky et al., 2007; 2010). This seismic activity shows that the
110 deformation between the Nubian and Somali plates is distributed over a wide area, in several
111 segments. In this complex tectonic setting, the exact location and the processes of deformation

related to plate tectonics movements in the area of the Mozambique Channel remain poorly understood. West of the Mozambique Channel, surface structural evidence for rifting appears to stop around 22°S, south of the Lake Malawi and the Inhaminga fault, in the Machaze epicentral area (Fig. 1), whereas seismic activity at depth extend farther to the south in Swaziland and South Africa (Fonseca et al., 2014). On the other hand, east of the Mozambique Channel, the presence of active volcanism, recent faults, and seismic activity suggest that active deformation running through wide parts of Madagascar might correspond to the western boundary of the Somali plate (Kusky et al., 2007, 2010; Stamps et al., 2008; Saria et al., 2013). Several authors have proposed the presence of a dominantly oceanic Lwandle block (name derived from the Xhosa word for ocean) extending south of the Rovuma block in the Mozambique Channel between southern Mozambique and Madagascar (Hartnady, 2002 ; Horner-Johnson et al., 2007 ; Stamps et al., 2008, 2018; Saria et al., 2014). The dimension and precise boundaries of this block are very poorly constrained at this stage. Kinematic models proposed by Stamps et al. (2008) and Saria et al. (2014) invoke a possible extensive/transform zone in the Mozambique channel distributed along a NE-SW trend crossing the channel (Figs. 1 and 2). Between Africa and Madagascar, the deep water area of the Mozambique basin is characterized by the development of an oceanic lithosphere which began to develop during the Mid Jurassic-Cretaceous drift of Antarctica with respect to Africa (Rabinowitz et al., 1983; Coffin and Rabinowitz, 1988). The oceanic domain of the Mozambique basin is largely invaded by sediments forming the turbidite system connected to the sediment supply coming from the Zambezi River (Walford et al., 2005). The main channel of this turbidite system shows locally strong evidence of erosion (Kolla et al., 1991). The Mozambique Channel is also characterized by the presence of the Davie ridge which runs NNW-SSE west of Madagascar and which delimits the eastern part the oceanic domain of the Mozambique Channel. It corresponds to the extinct transform fault system along which

137 Madagascar separated from the future Somali plate between 160–115 Ma ago. Dredge
138 samples collected along the Davie Ridge show that isolated blocks of Precambrian basement
139 and volcanics are preserved along this paleo-transform ridge. These volcanics include Late
140 Cretaceous and Cenozoic lava flows (De Wit, 2003; Courgeon et al., 2016, 2017). The
141 oceanic domain of the Mozambique Channel is also the site of volcanic edifices forming
142 seamounts covered by Neogene carbonate deposits forming locally modern reefs and emerged
143 lands at Bassas da India and Europa (Jorry et al., 2016; Courgeon et al., 2016, 2017). The
144 average elevation of the Mozambique basin is anomalously high with respect to its age even
145 taking into account the sedimentary and volcanic input (Castelino et al., 2016) and this
146 anomalously shallow area extends largely southwesterly to the southwest offshore of South
147 Africa (Nyblade and Robinson, 1994). This topographic anomaly, as well as the significance
148 of the volcanism discovered in this area remained both largely unexplained before this study.

149

150 **3. Methodology**

151

152 In this paper, we present seismic reflection data coupled with multibeam echosounder
153 acquisitions. Geophysical data were acquired in the Mozambique Channel in 2014 and 2015
154 during the PTOLEMEE (Jorry, 2014), PAMELA-MOZ02 (Robin and Droz, 2014) and
155 PAMELA-MOZ04 (Jouet and Deville, 2015) marine surveys aboard the RV *L'Atalante* and
156 *Pourquoi Pas?* The seismic source used for the seismic acquisitions was 2 GI air guns
157 (105/105 ci, 45/45 ci). The streamer had 48 seismic traces with inter-traces of 6.25 m and 4
158 hydrophones SFH with a spacing of 0.78 m per trace. The total length of the streamer was
159 531.6 m. Acquisition time was 9 seconds and the sampling frequency was 1 kHz. The seismic
160 acquisition system was a SEAL 428, V1.1 Patch 23. Seismic data were processed using
161 Ifremer QC-Sispeed software and integrated in Kingdom Suite software for the interpretation
162 of seismic profiles. A map of the fault zone was produced (Fig. 2), encompassing the spatial

163 distribution of active faults (i.e. faults expressed up to the seafloor) and sealed faults (i.e.
164 faults covered by sediments). Bathymetric data were acquired using the multibeam
165 echosounders Kongsberg EM122 (Frequency of 12 kHz) and EM710 (Frequency bandwidth
166 of 71-100 kHz). The data were processed using Ifremer Caraïbes software and integrated in
167 ArcGis software for morphobathymetric analysis of seafloor features. The map of the fault
168 zone based on seismic data was compared with morphobathymetric analysis.

169 In order to provide a reliable mapping of the fault zone, we compared the morphologic
170 features visible on bathymetric data and the visible structures on the seismic lines (Fig. 3), in
171 order to distinguish notably linear sedimentary features (e.g. dunes crests) and structural
172 lineaments (active faults; Fig. 3). The map of fault zone was completed for active faults
173 whose linear extent and orientation are visible on the bathymetric profiles (Fig. 3).

174

175 **4. Results and interpretation**

176

177 *4.1 Spatial distribution of the faults*

178

179 Several seismic profiles, especially around the Bassas da India and Europa islands, show the
180 presence of a wide system of faults (Fig. 2, 3). Some of the most characteristic lines
181 illustrating this fault system are presented in figure 4, 5, 6, and 7. The penetration in the
182 sediments is slightly than 1.5 s TWT (Two Way Travel time) and deepest observations reach
183 5.5 s TWT.

184 The results of the bathymetry-seismic reflection correlation are synthetized in Fig. 3 and
185 examples of the most characteristic bathymetric data showing morphologic expressions at the
186 seabedrelated to fault activity are shown along seismic lines of the Fig. 5 and 6. The
187 comparison between the morphological features visible on bathymetric data and the structures

visible on the seismic lines shows a good fit concerning the location of the fault system (Fig. 2, 5, 6). It also allows estimating the main strikes of the faults which is not possible with the seismic data alone because the density of the available seismic data does not allow correlating faults from one line to another. This combined approach using bathymetry and seismic data allows defining the main fracturing zones within the Mozambique Channel. This work shows that between latitudes 18°S and 20°S, the fault zone merges with the active fault system adjacent to the northern part of the Davie Ridge which has been described in recent papers (Mahanjane, 2014; Franke et al., 2015; Fig. 3), including notably, N-S trending faults found along the Sakalaves Mounts (Courgeon et al., 2018; Fig. 3). From the Davie ridge, the fault zone develops to the southwest across the Mozambique Channel. This fault zone, more than 200 km-wide, crosses the seamounts of Europa, Bassas da India, and Hall bank (Fig. 2, 4) and joins the northern part of the Mozambique Ridge to the southwest. Two main trends of fault strikes have been observed, one trending N160-180°, the other N45-80° (Fig. 2). This confirms the results of a recent study of the Mounts Sakalaves and the Bassas de India-Jaguar-Hall banks, which showed the existence of faults trending NE-SW that can be tracked on bathymetric data affecting the carbonates of the seamounts, some of these faults being associated with volcanic activity (Courgeon et al., 2016, 2017; Fig. 4). In the vicinity of the seamounts which include volcanic edifices, acoustic masks prevent these faults from being imaged under volcanic rocks (probably related to the contrast of the high seismic velocity of the volcanics compared to the seismic velocity of the sediments around; Fig. 7) but apart from seamounts, faults are clearly visible on the seismic reflection lines. The fault system is trending toward the southwest of the Mozambique Basin as a continuation of the Agulhas major fracture zone (Fig. 1), which extends largely westward along the Falkland fault zone in Southern Atlantic.

212 On some of the seismic lines considered approximately perpendicular to the strike of the
213 faults, depth-conversion with an average velocity of 2000 m/s (mean velocity deduced from
214 refraction studies and ODP drilling in the area, ODP leg 25, wells 242, 248, 250; see
215 Supplementary Material, Figs. S2 and S3) shows that most of these faults, north of the Europa
216 island, correspond to normal faults. Indeed, these faults have apparent conjugated dips
217 showing absolute values between 50° and 70° (Fig. 4, 5, 6, *i.e.* compatible with conjugated
218 normal faults). In the south of Europa Island, to the southwest, the faults tend to be steeper
219 and many of them are almost vertical (Fig. 7). As such, the fault system of this SW area is
220 different from the characteristic conjugated systems of normal faults present in the northern
221 part of the Mozambique Channel and the presence of nearly vertical faults suggests a strike-
222 slip activity. In addition, well-expressed and localized depressions forming traps for the
223 sediments of the Mozambique turbidite system may correspond to pull-apart basins associated
224 with strike-slip activity. This interpretation is consistent with the fact that some border faults
225 systems of these depressions show clear evidence for the development of en-échelons systems
226 of faults probably related to right lateral strike-slip component (Fig. 9). The general
227 characteristics of the fault geometries in the southwestern part of the Mozambique Channel
228 can be regarded as related to transtensional structures.

229 The most recent faults affect all sedimentary series down to the penetration window and
230 are well-expressed in the seabed topography with fault scarps up to 50 ms TWT visible on
231 both the seismic lines and multibeam data. It is therefore likely that these faults were active
232 during Quaternary times and some of them are probably active and contemporaneous with the
233 most recent volcanism events. The fault zone described here is indeed still partly active as
234 shown by the seismicity data in the Europa and Bassas da India area (Fig. 1; see discussion
235 below). The profile L4 in figure 6 shows a major syn-sedimentary fault with very high
236 amplitude reflectors in the shallow layers. The syn-tectonic character of this fault is

237 demonstrated by the presence of syn-tectonic pinch-out clearly visible on the seismic line
238 (Fig. 6). This fault, well-expressed in the topography of the sea bottom, is probably an active
239 fault. Throughout the study area, the major faults affect the sedimentary series down to the
240 penetration limit of the seismic data.

241 In addition to the faults that affect the uppermost sedimentary series many faults do not
242 reach the seabed. The interpretation of the timing of activity of these buried faults is
243 questionable. They can either correspond to sealed faults which were active in the past and
244 then became inactive after or, depending on the rheological properties of the sedimentary
245 series, some faults may be expressed at depth (brittle deformation), while deformation is
246 accommodated by continuous creeping in shallower layers. The observed offsets of the sealed
247 faults seem to be lower than the one of the active faults (maximum ~ 30 ms TWT, ~ 20 m) but
248 these faults are much more numerous than the recent faults (Fig. 5, 6, 7). This suggests that
249 early deformation was more diffuse and widely distributed and that, overtime, deformation
250 tended to be more localized. Some of these faults are hardly detectable (if at all) in a poorly
251 reflective interval (Fig. 5, 6, 7). This could be related to the rheological properties of these
252 levels which can correspond to relatively plastic clays-rich horizons. On the other hand, many
253 faults are sealed by the uppermost sedimentary series and partly by volcanic flows (Fig. 5, 6,
254 7).

255

256 *4.2 Chronostratigraphic framework of fault activity*

257

258 The picking of these faults shows that they are not always sealed at the same level but,
259 depending of the cases, the throw of the fault stops at different stratigraphic layers (Fig. 4). In
260 addition, in some cases, the values of the fault throw are higher at depth with some values
261 above 100 ms TWT. This suggests a relatively long duration of fault activity (since the

262 Miocene). It is worth noting that sealed faults are also observed on the inactive part of the
263 Davie Ridge (southernmost area of this ridge) as evidenced by the draping of faults by the
264 sediments (Fig. 5).

265 In order to propose a timing of the beginning of the fault activities, we picked some
266 characteristic horizons which are interpreted as time lines (Fig. 4, 5, 6, 7). The ages proposed
267 for these horizons are consistent with the interpretations of Franke et al. (2015) in the northern
268 part of the Mozambique Channel and Mahanjane et al. (2014b) and Ponte (2018) from well
269 calibration located on Zambezi platform (yellow marker: near top Miocene, orange marker:
270 near top Oligocene, red marker: near top Eocene). According to this interpretation, it appears
271 that all the faults affect Miocene and older sediments but some being sealed at the top of the
272 Miocene whereas, as mentioned previously, others affect the whole stratigraphic series up to
273 the sea-bottom. Accordingly, we deduced that the global period of faulting lasted from late
274 Miocene to present-day.

275

276 **5. Discussion**

277

278 *5.1. Structural trends within the fault zone*

279

280 Between the Davie Ridge and the Mozambique Ridge, the fault system developed within the
281 oceanic lithosphere of the Mozambique Basin (see Fig. 10, with location of the oceanic crust
282 from Konig and Jokat, 2010; Leinweber and Jokat, 2012; Davis et al., 2016; Mueller and
283 Jokat, 2017). In this area, the tectonic style is different from the dominant one north of 20°S
284 which corresponds to rift-related structures including the tilt of wide continental crustal
285 blocks (Franke et al., 2015). South of 20°S, the fault zone forms a wide area (> 200 km wide)
286 characterized by a diffuse deformation made of a relatively dense system of faults with

287 moderate throws. These faults are mostly straight (planar), whereas the main faults are mainly
288 listric north of 20°S (Franke et al., 2015). This may be due to the fact that the oceanic
289 lithosphere does not include decoupling layers like the lower thick continental crust, the
290 faults being here rooted deeply within the oceanic lithosphere.

291 Within this fault zone affecting the oceanic lithosphere of the Mozambique Basin, two main
292 strikes of fault were observed, N160-180° and NE-SW. The N160-180° trends are
293 predominant in the northern area (north of Bassas da India), while fault trends from the
294 southern area are mostly oriented NE-SW. These different trends are possibly controlled by
295 inherited fracture zones within the oceanic lithosphere, the N160-180° trends being probably
296 controlled mainly by transform fracture zones parallel to the Davie Ridge transform system
297 (Fig. 10), and the NE-SW trends being possibly influenced by fractures which are parallel to
298 the magnetic anomalies of the oceanic crust (normal faults from the oceanic accretion period;
299 Fig. 10).

300

301 5.2. *Active earthquakes along the fault zone*

302

303 A correlation exists between the area of recent faulting evidenced within the Pliocene-
304 Quaternary sediments and the location of the earthquakes (Fig. 10). Indeed, the most
305 significant earthquakes ($M_w > 4$) recorded within the Mozambique Channel are trending
306 mostly along the zones where the faults described in this paper are reaching the sea floor (Fig.
307 2). Only a few isolated and relatively shallow earthquakes (focal depths < 25 km) occurred
308 south of this fault zone in the deep water part of the Mozambique Basin south of 26°S (Fig.
309 10, see also supplementary material Fig. S1, Table S1). These isolated earthquakes show focal
310 mechanisms consistent with a NW-SE extension (Fig. 10), while earthquake focal
311 mechanisms north of Mozambique Channel along the Davie Ridge are consistent with

312 roughly a E-W extension with focal depths mostly shallower than 25 km, some being between
313 25 km and 50 km (Foster and Jackson, 1998; Yang and Chen, 2010; Saria et al., 2014; Fig. 2,
314 3). The 4 larger earthquakes (Mw 5.0 to 5.7) over the last 50 years were recorded between
315 1980 and 1983, in the Europa/Bassas da India region. In 1951 and 1950, earthquake
316 magnitudes reached Mw 6.1 and 6.2 in the area of the Davie Ridge (Fig. 2). South of 20°S,
317 the Davie Ridge is mostly tectonically inactive (no recorded earthquake > Mw 3 and no
318 evidence of recent tectonics on the seismic lines as shown by the fault sealing of the Ridge;
319 Fig. 2). As mentioned above, to the southwest, the studied active fault zone seems to be
320 aligned with Agulhas-Falkland fault zone where important earthquakes have been mentioned,
321 notably one Mw 6.8 located offshore of Durban in the Natal valley (point A in Fig. 1), which
322 occurred December 31st, 1932 (focal depth 15 km). This area of the Natal valley is possibly
323 associated with volcanic seamounts which might be related to the EARS extension tectonics
324 (Wiles et al., 2014). The active fault system described in this paper which is associated to
325 seismic activity is clearly distinct from the deformation trend onshore Mozambique which is
326 associated to seismic activity characterizing an E-W extension or local strike-slip movements
327 (Fig. 10). It is also clearly distinct from the deformation processes recorded within
328 Madagascar which are associated to scattered earthquakes some of them being compressional
329 (Fig. 10).

330

331 *5.3. Fault zone and volcanism*

332

333 As described in previous works, the carbonate seamounts of the Mozambique Channel
334 have developed either on crystalline basement rocks or on volcanic systems (Bassias, 1992;
335 Courgeon et al., 2016, 2017). Faults are expressed at the seabed even in the most recent
336 carbonate deposits covering the volcanic edifices (Figs. 4 and 7). The main volcanic edifices

337 trending along the fault zone described in this work were most likely developed during Mid-
338 Miocene but volcanism went on to be active until very recent times forming dykes and lava
339 flows visible at the sea bottom (Courgeon et al., 2016, 2017). The acoustic masks below the
340 volcanics around Bassas da India, Europa Islands and Hall Bank being located along the fault
341 zone, we can assume that the volcanic mounts are rooted on deep faults that cannot be imaged
342 from the seismic data because of the acoustic mask under the volcanics. In the peripheral
343 areas of the Mozambique Channel, the end of the Miocene corresponds to a period of
344 significant volcanism, probably the major episode in the region (Roberts et al., 2012).
345 Therefore, some of the faults were probably already active as soon as Miocene times which is
346 consistent with the tectonic framework of the EARS (Chorowicz, 2005; McGregor, 2015).

347

348 *5.4. Significance of the fault zone in the framework of plate tectonics*

349

350 In terms of global plate tectonics and location of deformation zones between the Nubian
351 and Somali plates, this study shows that one of the branches of this complex plate boundary
352 (the eastern branch of the EARS) can be followed at least as south as 25°S trending toward
353 the area where most of the kinematic studies locate the pole of rotation between Nubia and
354 Somalia plates (see discussion above § 2; Fig. 1). As such, this study shows that the eastern
355 branch of the East African Rift System is extending much further south than previously
356 demonstrated with facts, not only in continental domains but also across the oceanic
357 lithosphere of the Mozambique basin. As it is the case along the eastern branch of the EARS
358 north of the studied area (Mulibo and Nyblade, 2013), the zone of lithospheric divergence
359 presented in this paper, with a transform component toward the south, is probably responsible
360 for the thinning and the rise of the mantle below which may be the cause of partial melting in
361 the mantle sourcing the volcanic systems associated with the fault zone. This oceanic mantle

362 rise is also probably responsible for the regional uplift linked with the anomalously high
363 topography of the northern part of the Mozambique basin mentioned previously.

364

365 **6. Conclusion**

366

367 This study has shown that the eastern branch of the EARS extends offshore across the
368 Mozambique Channel from the Davie Ridge to the Mozambique Ridge, where it is
369 characterized by a zone of densely distributed faults, trending NNE-SSW and deforming the
370 oceanic lithosphere of the Mozambique channel that developed much earlier, during Jurassic-
371 Cretaceous times. The fault zone is well characterized within the sediments of the
372 Mozambique basin and shows that faults have been active since at least the Miocene times
373 and some of them are still seismically active (Fig. 10). Earthquakes with magnitude reaching
374 Mw 6.1 around the Davie Ridge and Mw 5.7 around the Europa-Bassas da India Islands
375 occurred along the fault zone during the last decades. The focal depths of the earthquakes are
376 deeper than the sedimentary accumulations, probably within the mantle of the oceanic
377 lithosphere of the Mozambique Basin. The fault zone structure is compatible with a purely
378 extensional deformation around the Davie Ridge and a dextral transtensional system between
379 the Davie Ridge and the Mozambique Ridge. This interpretation is also compatible with
380 earthquake focal mechanisms (Fig. 10) and recently published kinematic models (Stamps et
381 al., 2008; 2014, 2018; Saria et al., 2014). The fault zone activity is associated with volcanic
382 activity controlling the development of the seamounts present within the Mozambique
383 Channel. This active extensional process taking part of the EARS is probably associated with
384 mantle rise that might be responsible for the anomalously high topography of the northern
385 part of the Mozambique basin due to the presence of relatively hot rising mantle at depth.
386 With active deformation onshore Africa, notably along the Inhaminga fault zone, and also

387 along the Comoros-Mayotte and Madagascar system, the active fault zone of the Mozambique
388 Channel is participating to the complex plate boundary between the African main continent
389 (Nubia Plate) and Madagascar (Somalia Plate).

390

391 **Acknowledgements**

392

393 This work has been conducted within the framework of the PAMELA (PAssive Margin
394 Exploration LABoratories) project leaded by IFREMER and TOTAL in collaboration with
395 Université de Bretagne Occidentale, Université de Rennes 1, Université Pierre et Marie Curie
396 Paris 6, CNRS and IFP Energies Nouvelles. Data acquisition was made in 2014 during the
397 PTOLEMEE (Jorry, 2014), and PAMELA-MOZ02 (Robin and Droz, 2014) marine surveys
398 onboard the R/V *L'Atalante* and in 2015 during the PAMELA-MOZ04 survey (Jouet and
399 Deville, 2015) onboard the R/V *Pourquoi Pas?* We thank captains, officers, crew members
400 and scientific teams of the PTOLEMEE, PAMELA-MOZ2 and PAMELA-MOZ4 cruises for
401 their technical support in recovering dataset. Yannick Thomas and Pauline Dupont from
402 Ifremer are acknowledged for their contribution in the processing of the seismic lines.

403

404

405 **Appendix A. Supplementary data**

406

407 Supplementary data to this article can be found at <http://www.seanoe.org/data/00445/55634/>
408 (Licence: Creative Commons Attribution, no commercial usage, sharing under the same
409 conditions).

410

411

412 **References**

- 413
- 414 Altamimi, Z., Métivier, L., Collilieux, X., 2012. ITRF2008 plate motion model, *J. Geophys.*
415 *Res.*, 117, B07402, doi:10.1029/2011JB008930.
- 416 Argus, D. F., R. G. Gordon, M. B. Heflin, C. Ma, R. Eanes, P. Willis, W. R. Peltier, and S.
417 Owen (2010), The angular velocities of the plates and the velocity of Earth's center from
418 space geodesy, *Geophys. J. Int.*, 180(3), 916–960, doi:10.1111/j.1365-246X.2009.04463.x.
- 419 Bassias, Y., 1992. Petrological and geochemical investigation of rocks from the Davie
420 fracture zone (Mozambique Channel) and some tectonic implications, *J. Afr. Earth Sci.*
421 (Middle East), 15(3–4), 321–339.
- 422 Bertil, D., Regnoult, J.M., 1998. Seismotectonics of Madagascar. *Tectonophysics* 294, 57-74.
- 423 Calais, E., Hartnady, C., Ebinger, C., Nocquet, J. M., 2006. Kinematics of the East African
424 Rift from GPS and earthquake slip vector data, in Structure and Evolution of the Rift
425 Systems Within the Afar Volcanic Province, Northeast Africa, *Geol. Soc. London Spec.*
426 *Publ.*, vol. 259, edited by G. Yirgu, C. J. Ebinger, and P. K. H. Maguire, 9–22.
- 427 Castelino, J.A., Eagles, G., Jokat, W., 2016. Anomalous bathymetry and palaeobathymetric
428 models of the Mozambique Basin and Riiser Larsen Sea. *Earth and Planetary Science*
429 *Letters* 455, 25-37.
- 430 Chorowicz, J., 2005. The East African rift system. *Journal of African Earth Sciences* 43(1–3),
431 379–410.
- 432 Chu, D., Gordon, R.G., 1999. Evidence for motion between Nubia and Somalia along the
433 Southwest Indian Ridge, *Nature*, 398, 64– 67.
- 434 Coffin, M. F., Rabinowitz, P.D., 1987. Reconstruction of Madagascar and Africa: Evidence
435 from the Davie Fracture Zone and Western Somali Basin, *J. Geophys. Res.*, 92(B9), 9385–
436 9406, doi:10.1029/JB092iB09p09385.

- 437 Courgeon S., Jorry, S.J., Camoin, G.F., BouDagher-Fadel, M.K., Jouet G., Révillon, S.,
438 Bachèlery, P., Pelleter, E., Borgomano, J., Poli, E., Droxler, A.W., 2016. Growth and
439 demise of Cenozoic isolated carbonate platforms: New insights from the Mozambique
440 Channel seamounts (SW Indian Ocean). *Marine Geology* 380, 90–105.
- 441 Courgeon, S., Jorry, S.J., Jouet, G., Camoin, G., Bou Dagher-Fadel, M.K., Bachèlery, P.,
442 Caline, B., Boichard, R., Révillon, S., Thomas, Y., Thereau, E., Guérin, C., 2017. Impact
443 of tectonic and volcanism on the Neogene evolution of isolated carbonate platforms (SW
444 Indian Ocean). *Sedimentary geology* 355, 114-131.
- 445 Davis, J.K., Lawver, L.A., Norton, I.O., Gahagan, L.G., 2016. New Somali Basin magnetic
446 anomalies and plate model for the early Indian Ocean. *Gondwana Research* 34, 16-28.
- 447 DeMets, C, Gordon R.G., Argus D.F., 2010. Geologically current plate motions, *Geophys. J. Int.*, 181, 1–80, doi:10.1111/j.1365-246X.2009.04491.xDelvaux, D., Barth, A., 2010.
448 African stress pattern from formal inversion of focal mechanism data. *Tectonophysics*
449 482(1),105-128.
- 450 Domingues, A., Silveira, G., Ferreira A.M.G., Chang S.-J., Custodio S., , Fonseca, F.B.D.J.,
451 2016. Ambient noise tomography of the East African Rift in Mozambique *Geophys. J. Int.*
452 204, 1565–1578 doi: 10.1093/gji/ggv538
- 453 Ebinger, C., 2012. Evolution of the Cenozoic East African Rift System: Cratons, plumes, and
454 continental breakup, in *Regional Geology and Tectonics: Phanerozoic Rift Systems and*
455 *Sedimentary Basins*, edited by D. G. Bally and A. W. Roberts, 132–162, Elsevier, Boston.
- 456 Ekström, G., Nettles, M., Dziewoński, A.M., 2012. The global CMT project 2004–2010:
457 Centroid-moment tensors for 13,017 earthquakes, *Phys. Earth Planet. Inter.*, 200–201, 1–9.
- 458 Emerick, C. M., Duncan, R.A., 1982. Age progressive volcanism in the Comores
459 Archipelago, western Indian Ocean and implications for Somali plate tectonics, *Earth*
460 *Planet. Sci. Lett.*, 60(3), 415–428.

- 462 Fernandes, R.M.S., Miranda, J.M., Delvaux, D., Stamps, D.S., Saria, E. 2013. Re-evaluation
463 of the kinematics of Victoria Block using continuous GNSS data. *Geophys. J. Int.* 193, 1–
464 10.
- 465 Fonseca J.F., Chamussa, J., Domingues, A.L., Helffrich, G., Antunes, E., van Aswegen, G.,
466 Pinto, L.V., Custódio, S., Manhiça, V. J., 2014. MOZART: A Seismological Investigation
467 of the East African Rift in Central Mozambique. *Seismological Research Letters Volume*
468 85, Number 1, January/February 2014, doi: 10.1785/0220130082
- 469 Foster, A.N., Jackson, J.A., 1998. Source parameters of large African earthquakes:
470 Implications for crustal rheology and regional kinematics, *Geophys. J. Int.*, 134(2), 422–
471 448.
- 472 Franke, D., W. Jokat, S. Ladage, H. Stollhofen, J. Klimke, R. Lutz, E. S. Mahanjane, A.
473 Ehrhardt, B. Schreckenberger, 2015. The offshore East African Rift System: Structural
474 framework at the toe of a juvenile rift, *Tectonics*, 34, 2086–2104,
475 doi:10.1002/2015TC003922.
- 476 Grimison, N.L., Chen, W.P., 1988. Earthquakes in Davie Ridge-Madagascar region and the
477 southern Nubian-Somalian plate boundary, *J. Geophys. Res.*, 93, 10,439–10,450.
- 478 Hartnady, C.J.H., 2002. Earthquake hazard in Africa: perspectives on the Nubia–Somalia
479 boundary. *South African Journal of Science* 98, 425–428.
- 480 Horner-Johnson, B. C., Gordon, R.G., Argus, D.F., 2007. Plate kinematic evidence for the
481 existence of a distinct plate between the Nubian and Somalian plates along the Southwest
482 Indian Ridge, *J. Geophys. Res.*, 112, B05418, doi:10.1029/2006JB004519.
- 483 Jorry, S., 2014. PTOLEMEE cruise, RV L'Atalante, <http://dx.doi.org/10.17600/14000900>.
- 484 Jorry, S.J., Camoin, G.F., Jouet, G., Le Roy, P., Vella, C., Courgeon, S., Prat, S., Fontanier,
485 C., Paumard, V., Boulle, J., Caline, B., Borgomano, J., 2016. Modern sediments and

- 486 Pleistocene reefs from isolated carbonate platforms (Iles Eparses, SW Indian Ocean): A
487 preliminary study. *Acta Oecol.* 72, 129–143.
- 488 Jouet, G., Deville, E., 2015. PAMELA-MOZ04 cruise, RV Pourquoi Pas?.
489 <http://dx.doi.org/10.17600/15000700>.
- 490 Kolla, V., Kostecki, J. A., Henderson, L., Hess, L., 1991. Morphology and Quaternary
491 Sedimentation of the Mozambique Fan and Environs, Southwestern Indian Ocean, in
492 Deep-Water Turbidite Systems (ed. D.A.V. Stow), Blackwell Publishing Ltd., Oxford, UK.
493 doi: 10.1002/9781444304473.ch36
- 494 Konig, M., Jokat, W., 2010. Advanced insights into magmatism and volcanism of the
495 Mozambique Ridge and Mozambique Basin in the view of new potential field data.
496 *Geophys. J. Int.* 180, 158–180. Doi: 10.1111/j.1365-246X.2009.04433.x.
- 497 Kusky, T.M., Toraman, E., Raharimahefa, T., 2007. The Great Rift Valley of Madagascar: an
498 extension of the Africa–Somali diffuse plate boundary? *Gondwana Research* 11, 577–579.
- 499 Kusky, T.M., Toraman, E., Raharimahefa, T., Rasoazanamparany, C., 2010. Active tectonics
500 of the Alaotra-Ankay Graben system, Madagascar: possible extension of Somalian-African
501 diffuse plate boundary. *Gondwana Res.* 18, 274–294.
- 502 Leinweber, V.T., Jokat, W., 2012. The Jurassic history of the Africa–Antarctica corridor—
503 new constraints from magnetic data on the conjugate continental margins. *Tectonophysics*
504 530–531, 87–101.
- 505 Mahanjane, E.S., 2014a. The Davie Fracture Zone and adjacent basins in the offshore
506 Mozambique Margin—A new insights for the hydrocarbon potential, *Mar. Pet. Geol.*, 57,
507 561–571.
- 508 Mahanjane, E. S., Franke, D., Lutz, R., Winsemann, J., Ehrhardt, A., Berglar, K., Reichert, C.,
509 2014b. Maturity and petroleum systems modelling in the offshore Zambesi Delta
510 depression and Angoche Basin, northern Mozambique, *J. Pet. Geol.*, 37(4), 329–348.

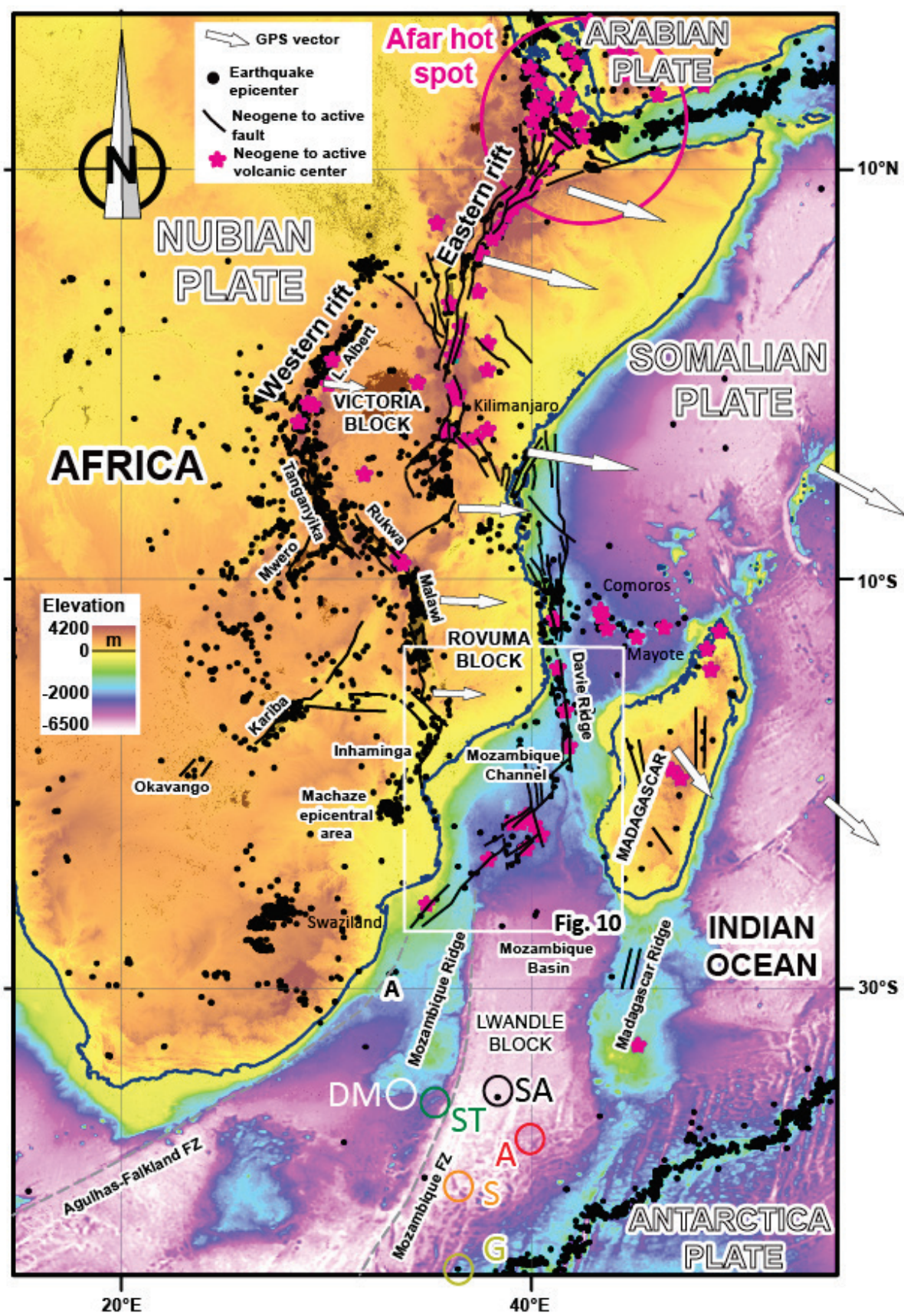
- 511 McGregor, D., 2015. History of the development of the East African Rift System: a series of
512 interpreted maps through time. *African Earth Sciences. J. Afr. Earth Sci.* 101, 232–252.
- 513 Michon, L., 2016. The volcanism of the Comoros Archipelago integrated at a regional scale.
514 In: Bachèlery, P., Lénat, J.-F., Di Muro, A., Michon, L. (Eds.), *Active Volcanoes of the*
515 *Southwest Indian Ocean*. Springer-Verlag, the Netherlands, 333–344.
- 516 Mougenot, D., Recq, M., Virlogeux, P., Lepvrier C., 1986. Seaward extension of the East
517 African Rift, *Nature*, 321(6070), 599–603.
- 518 Mueller, C.O., Jokat, W., 2017. Geophysical evidence for the crustal and distribution of
519 magmatism along the central coast of Mozambique. *Tectonophysics* 712-713, 684-703.
- 520 Mulibo, D.G., Nyblade, A.A., 2013. Mantle transition zone thinning beneath eastern Africa:
521 Evidence for a whole-mantle superplume structure. *Geophysical Research Letters*, 40,
522 3562–3566, doi:10.1002/grl.50694.
- 523 Mulibo, D.G., Nyblade, A.A., 2015. The seismotectonics of Southeastern Tanzania:
524 Implications for the propagation of the eastern branch of the East African Rift.
525 *Tectonophysics* 674, 20-30. doi:10.1016/j.tecto.2016.02.009.
- 526 Nyblade, A.A., Robinson, S.W., 1994. The African Superwell. *Geophysical Research Letters*,
527 21, 9, 765-768.
- 528 Ponte, J.-P., 2018. La marge africaine du Canal du Mozambique (le Système turbiditique du
529 Zambèze) : une approche « Source to Sink » au Méso-Cénozoïque. PhD Thesis, Rennes 1
530 University, 351 p.
- 531 Rabinowitz, P. D., Coffin, M., Falvey, D., 1983. The separation of Madagascar and Africa,
532 *Science*, 220, 67–69.
- 533 Reeves, C., 2014. The position of Madagascar within Gondwana and its movements during
534 Gondwana dispersal, *J. Afr. Earth Sci.*, 94, 45–57.

- 535 Roberts, E. M., Stevens, N.J., O'Connor, P.M., Dirks, P.H.G.M., Gottfried, M.D., Clyde,
536 W.C., Armstrong, R.A., Kemp, A.I.S., Hemming, S., 2012. Initiation of the western branch
537 of the East African Rift coeval with the eastern branch, *Nat. Geosci.*, 5(4), 289–294.
- 538 Robin, C. and Droz, L., 2014. PAMELA-MOZ2 cruise, RV L'Atalante.
539 <http://dx.doi.org/10.17600/14001100>.
- 540 Saria, E., Calais, E., Altamimi, Z., Willis, P., Farah, H., 2013. A new velocity field for Africa
541 from combined GPS and DORIS space geodetic solutions: Contribution to the definition of
542 the African reference frame (AFREF). *J. Geophys. Res. Solid Earth*, 118, 1677–
543 1697, doi:10.1002/jgrb.50137.
- 544 Saria, E., Calais, E., Stamps, D.S., Delvaux, D., Hartnady, C.J.H., 2014. Present-day
545 kinematics of the East African Rift, *Journal of Geophysical Research, Solid Earth*, 119,
546 3584–3600, doi:10.1002/2013JB010901.
- 547 Stamps, D.S., Calais, E., Saria, E., Hartnady, C., Nocquet, J.M., Ebinger, C.J., Fernandes,
548 R.M., 2008. A kinematic model for the East African Rift. *Geophysical Research Letters*,
549 35, L05304, doi:10.1029/2007GL032781, 2008
- 550 Stamps, D.S., Flesch, L.M., Calais, E., Ghosh, A., 2014. Current kinematics and dynamics of
551 Africa and the East African Rift System, *J. Geophys. Res. Solid Earth*, 119, 5161–5186,
552 doi:10.1002/2013JB010717.
- 553 Stamps, D.S., Saria, E., Kreemer, C., 2018. A Geodetic Strain Rate Model for the East
554 African Rift System. *Scientific Reports*. 8:732, DOI:10.1038/s41598-017-19097-w.
- 555 Storey, M., Mahoney, J.J., Saunders, A.D., Duncan, R.A., et al., 1995. Timing of hot spot-
556 related volcanism and the breakup of Madagascar and India. *Science* 267 (5199), 852.
- 557 Suess, E., 1891. Die Brüche des östlichen Africa. In: Beiträge zur Geologischen Kenntnis des
558 östlichen Africa, Denkschriften Kaiserlichen Akademie der Wissenschaftliche Klasse,
559 Wien 50, 555–556.
- 560 Walford, H. L., White, N.J., Sydow, J. C., 2005. Solid sediment load history of the Zambezi
561 Delta, *Earth Planet. Sci. Lett.*, 238(1–2), 49–63.

- 562 Wiles, E., Green, A., Watkeys, M., Jokat, W., Krocker, R., 2014. Anomalous sea floor
563 mounds in the northern Natal Valley, southwest Indian Ocean: Implications for the East
564 African Rift System. *Tectonophysics* 630, 300-312.
- 565 De Wit, M.J., 2003. Madagascar: Heads It's a Continent, Tails It's an Island. *Annual Review of Earth and Planetary*
566 *Sciences* 31, 2003 213-248.
- 567 Yang, Z., Chen, W.-P., 2010. Earthquakes along the East African Rift System: A multiscale,
568 system-wide perspective. *Journal of Geophysical Research*, 115, B12309,
569 doi:10.1029/2009JB006779.
- 570

571 Figures

572



573

574

575 **Fig. 1.** Location of the study area in the context of plate boundary between the Nubian and
576 Somali plates. Elevation/bathymetry grid from GEBCO. Black dots represent earthquake
577 epicenters from the NEIC catalog (USGS). Black lines represent major faults along the EARS
578 (compilation from Chorowicz, 2005; McGregor et al., 2015 on land; Franke et al., 2015 and
579 this study offshore). Vectors show GPS velocities in a Nubia-fixed reference frame from Saria
580 et al. (2013). The location of the rotation poles of Nubia *versus* Somalia are from Stamps et
581 al., 2008 (ST), DeMets et al., 2010 (DM), Argus et al., 2010 (G), Altamimi et al., 2012 (A),
582 Saria et al., 2013 (S), Saria et al., 2014 (SA). The Victoria, Rovuma and Lwandle plate are
583 considered by these authors as relatively rigid poorly deformed blocks between the Nubia and
584 Somalia plates. The limits of the Lwandle plate are poorly constrained by structural data.
585 Point A corresponds to the location of the 31/12/1932 M 6.8 earthquake offshore South
586 Africa.

587

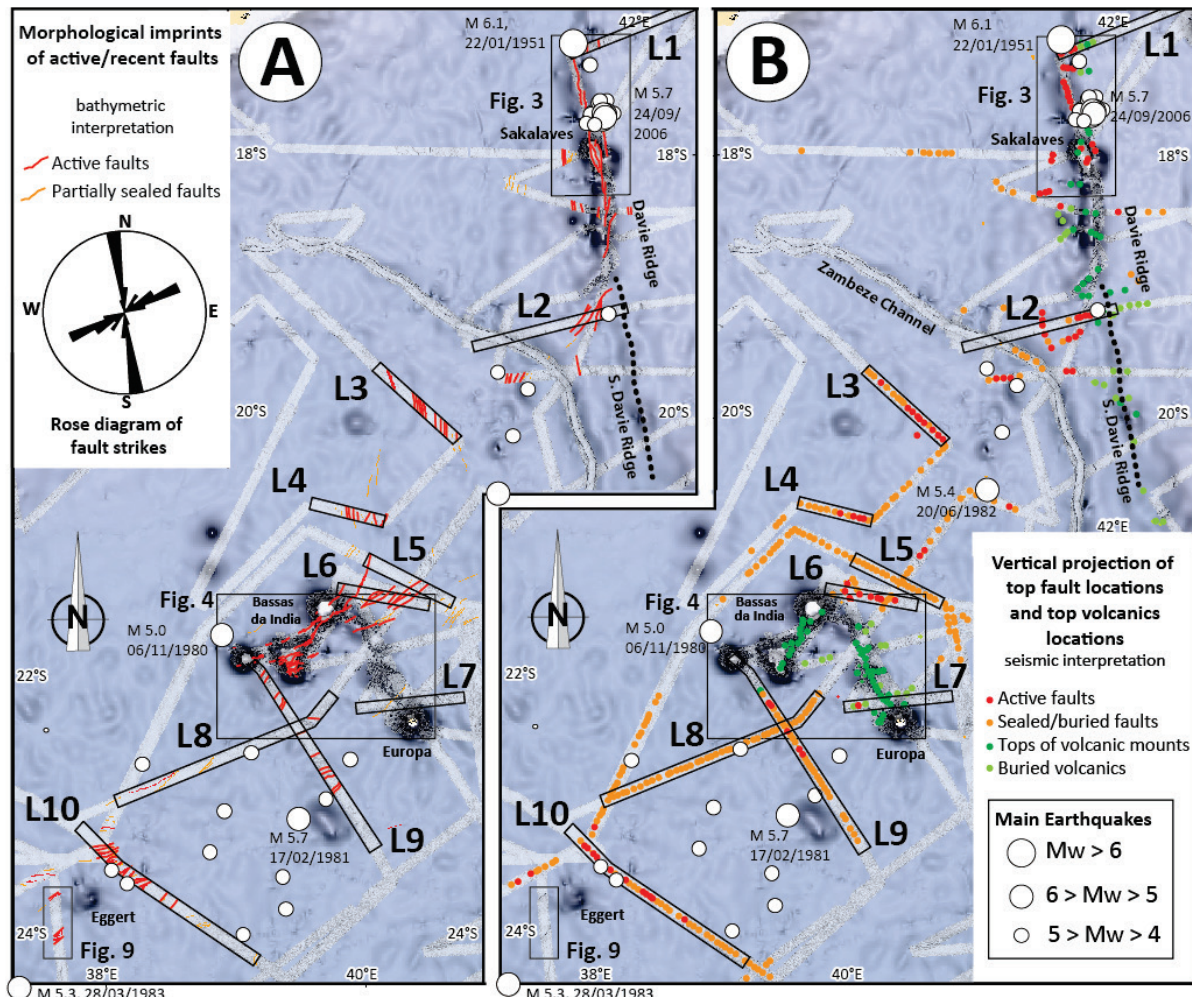
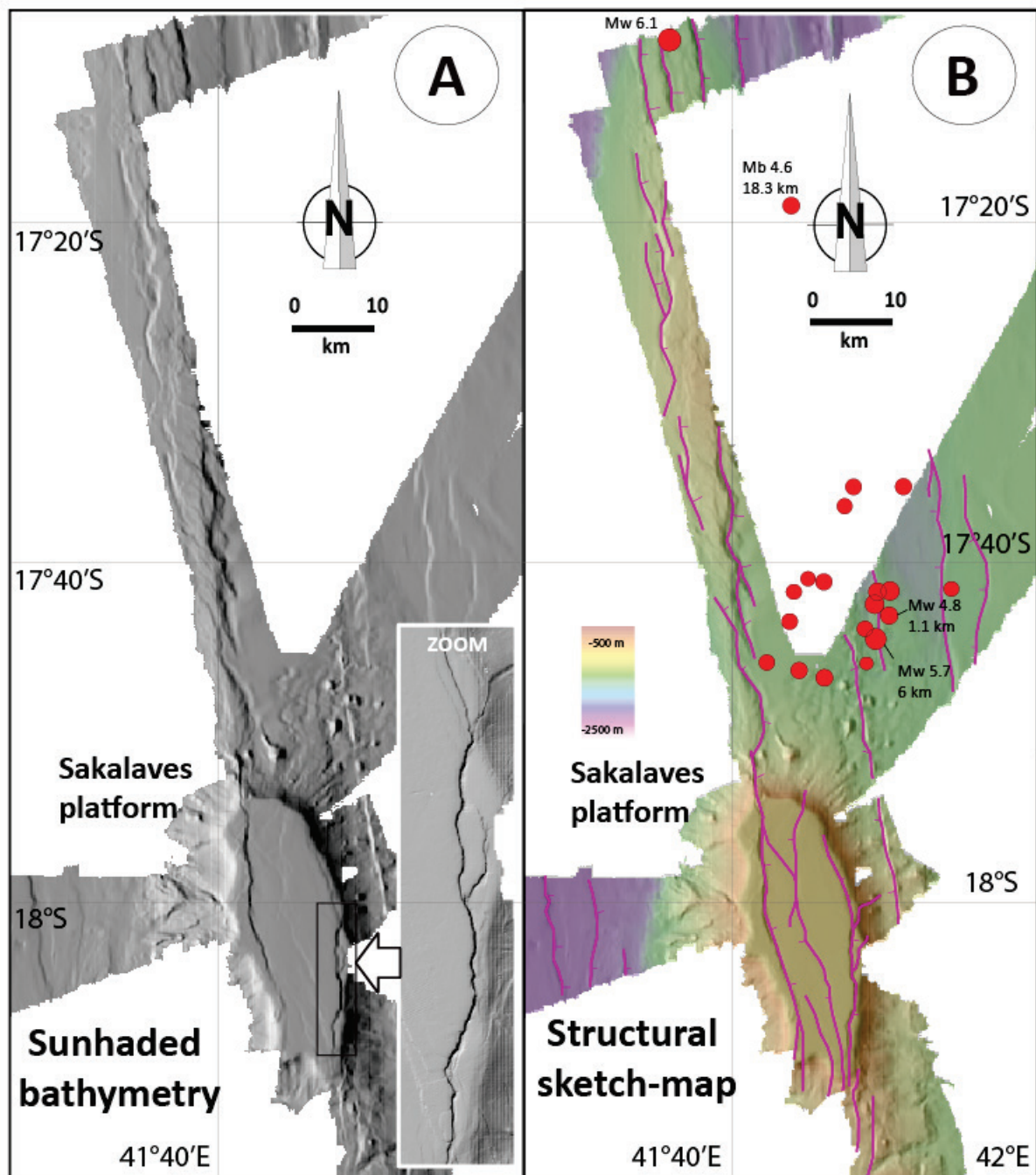


Fig. 2. Spatial distribution of faults in the Mozambique Channel. **(A)** Map showing the main faults visible at the sea bottom on multibeam data and rose diagram showing the preferential orientation of these faults. **(B)** Map showing the vertical projection at the sea floor of the top of the main faults and volcanic mounts interpreted on the vertical seismic data. Rectangles correspond to the location of figures 3, 4 and 9. L1 to L10 correspond to the location of the seismic profiles shown in figures 5 to 8. The comparison between map A and map B shows a very good fit for the location of the active fault zones in the area. The location of the faults is consistent with the location of the main earthquakes epicenters. The location of the piercing

599 volcanic spots is located along the active fault zones. Note also that the southern part of the
600 Davie Ridge shows no evidence of active faulting or volcanism.

601

602

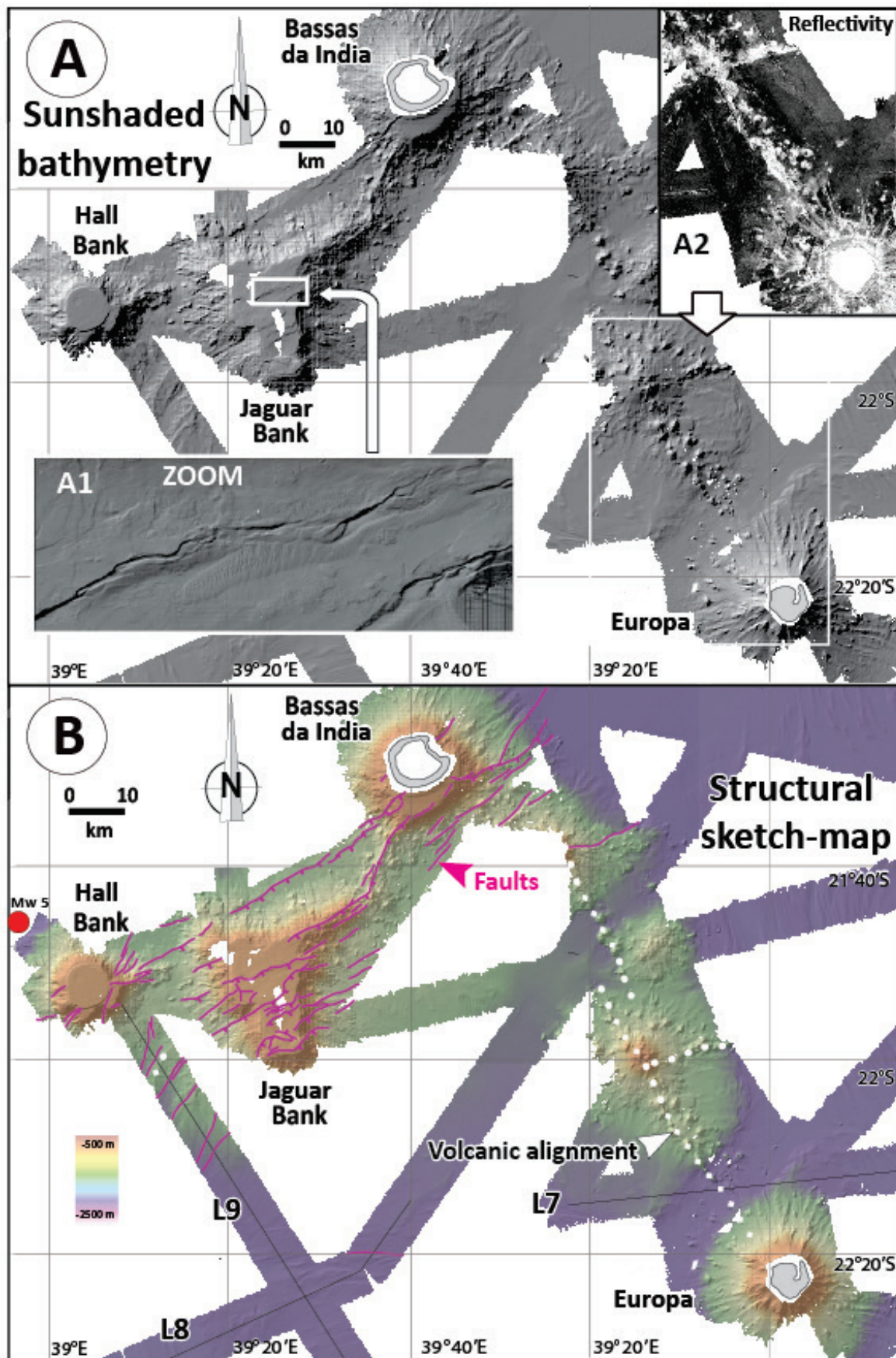


603

604

605 **Fig. 3.** Sunshaded bathymetry (A) and interpretative structural sketch-map (B) showing the
 606 fault pattern in the Sakalaves area. Dashes along faults indicate the down-thrown
 607 compartments.

608

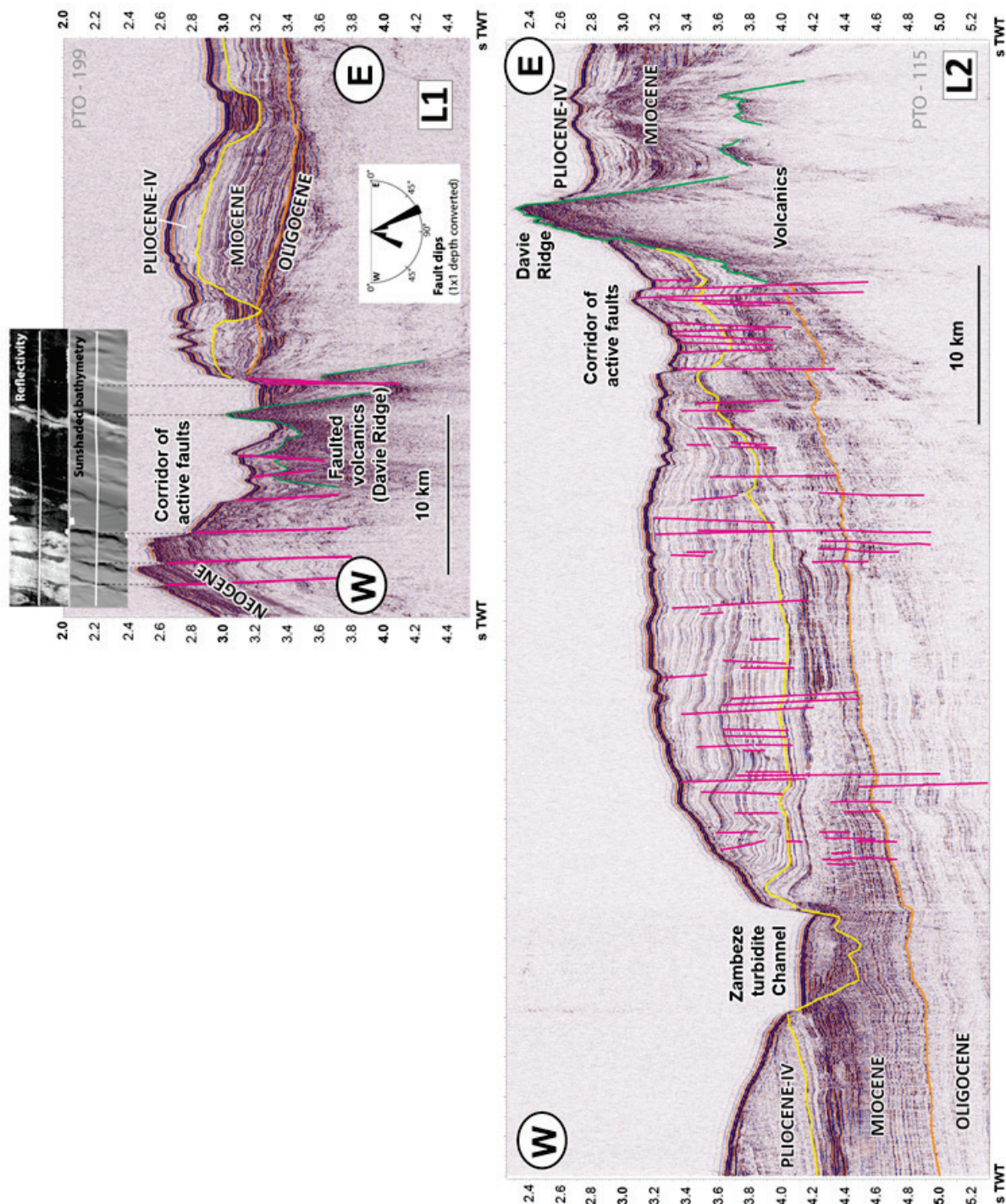


609

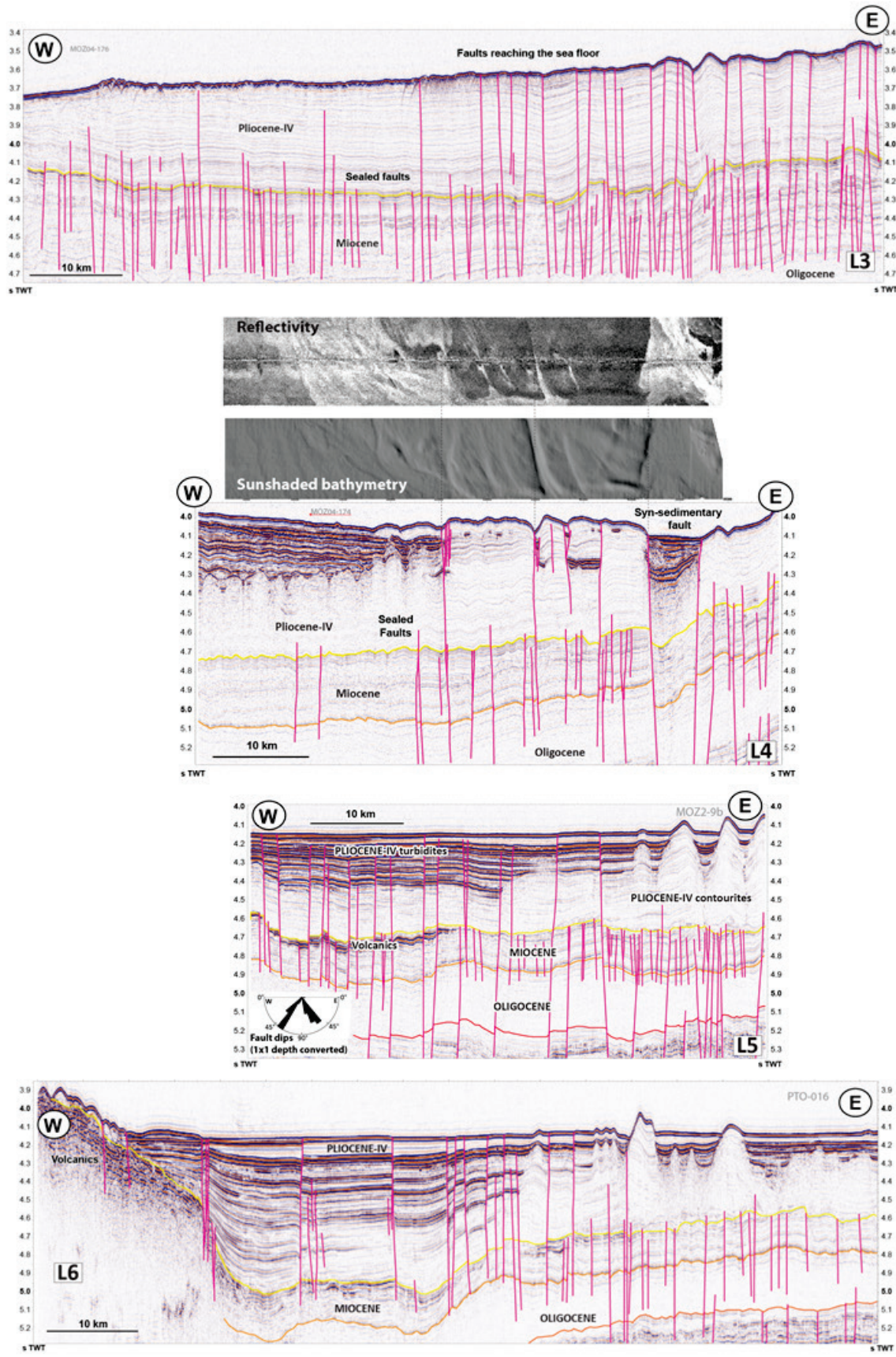
610

611 **Fig. 4. (A)** Sunshaded bathymetry of the Bassas da India and Europa area. A1 is a zoom
612 focusing on morphologic evidence of faults at the sea bottom. A2 corresponds to the
613 reflectivity map outlining the volcanic alignments north-west of Europa. **(B)** Interpretative
614 structural sketch-map showing the fault pattern in the Bassas da India and Europa area
615 (modified from Courgeon et al., 2016, 2017). Dashes along faults indicate the down-thrown
616 compartments.

617



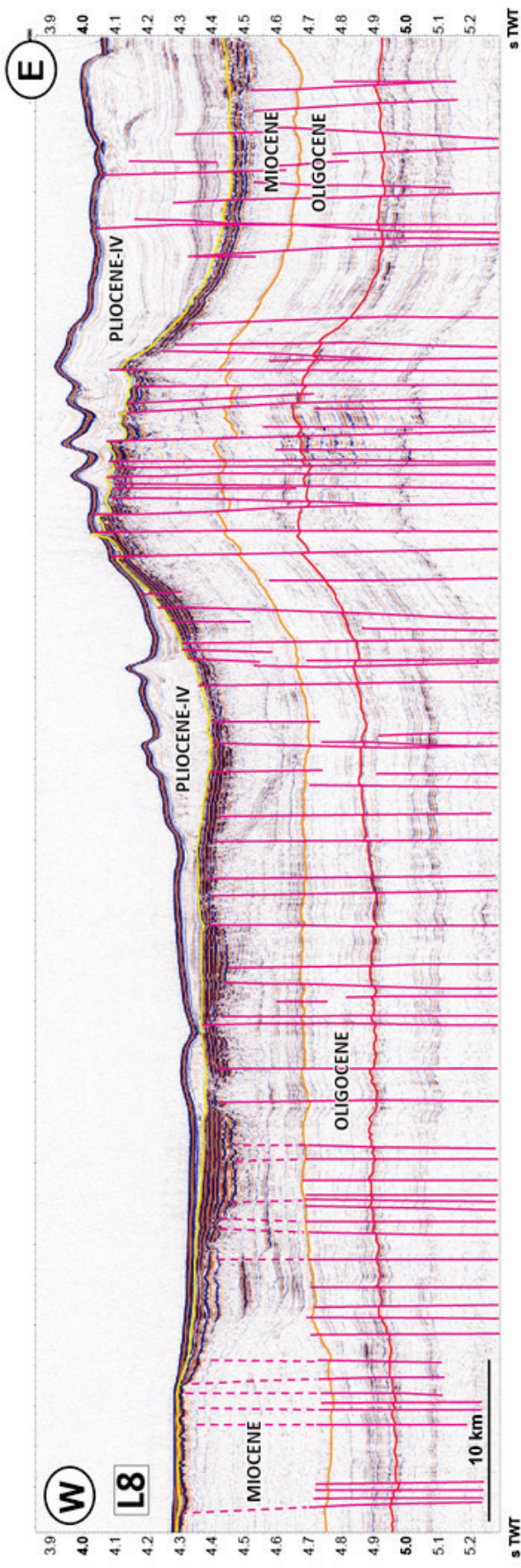
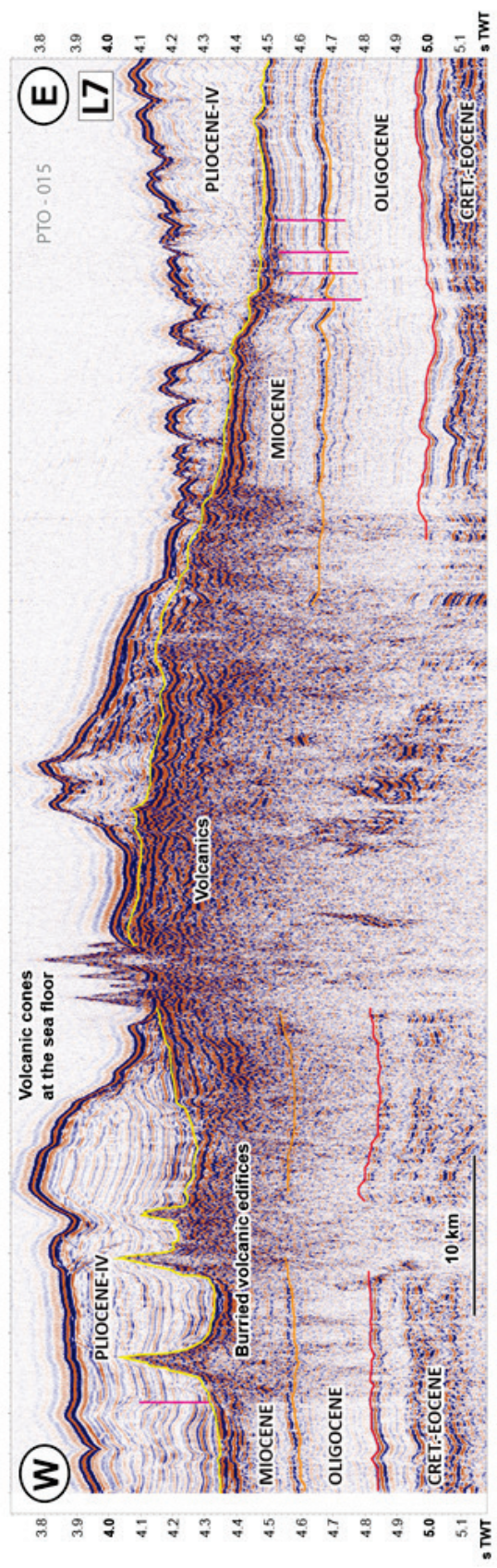
621 **Fig. 5.** Seismic profiles L1 and L2 illustrating the fault zone system of the Mozambique
622 Channel in the area of the Davie Ridge. Location of L1 and L2 in figure 2.
623



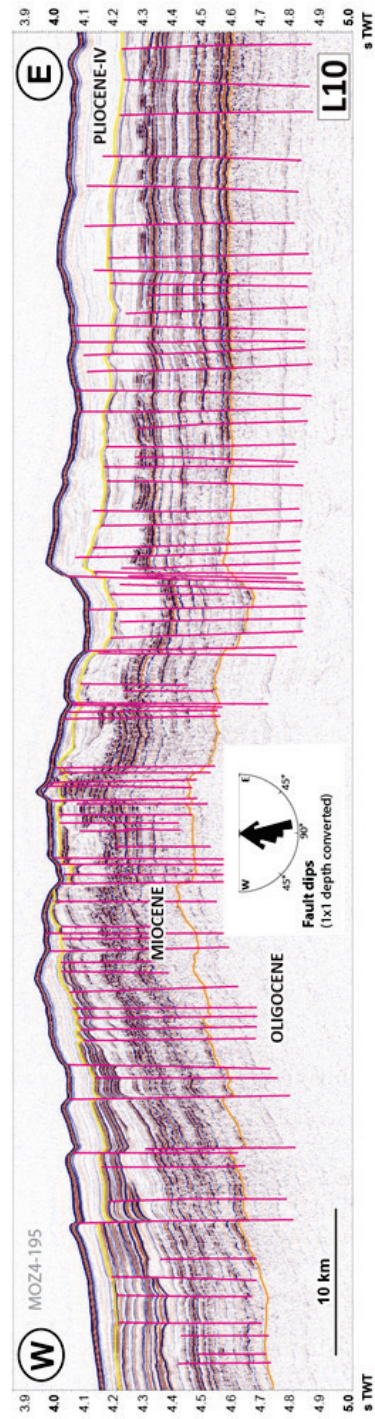
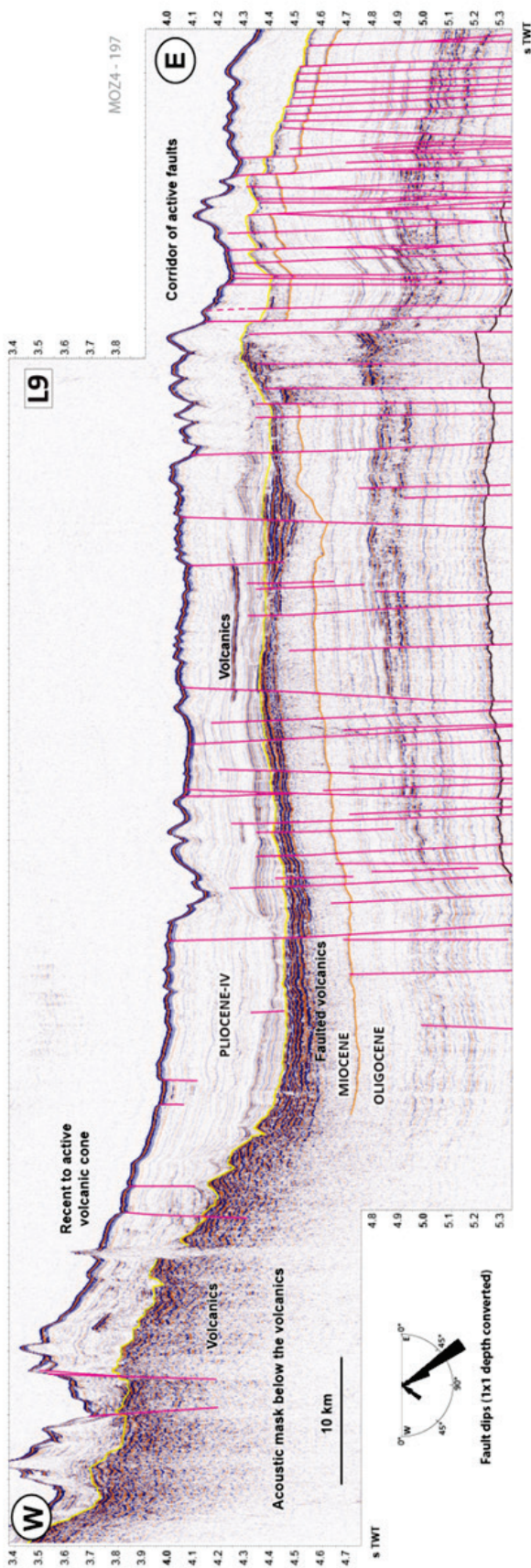
625 **Fig. 6.** Seismic profiles illustrating the fault zone system of the Mozambique Channel north of

626 Bassas da India (profiles location in figure 2).

627



629 **Fig. 7.** Seismic profiles South of Bassas da India (profiles L8 and L7 located in figure 2). L7
630 illustrates the presence of volcanic systems and deeply buried seamounts. L8 shows local
631 folding and uplift at least of the pre-Pliocene sediments.

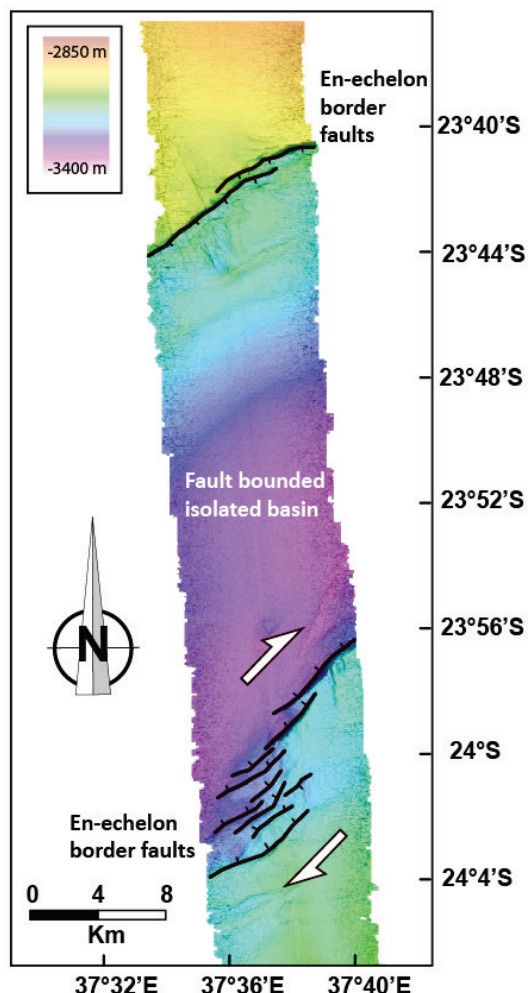


634 **Fig. 8.** Seismic profiles illustrating the fault zone system of the Mozambique Channel south
635 of Bassas da India (profiles L9 and L10 located in figure 2). Profile L9 illustrates the
636 relationship between the fracture network and volcanic activity. The faults expressed at the
637 bottom of the sea are recent to active whereas the faults sealed by the superficial sediments
638 indicate a stoppage of their functioning. Note the presence of a volcanic peak and a volcanic
639 unit marked by very high amplitudes which covers the older sedimentary series.

640

641

642



643

644

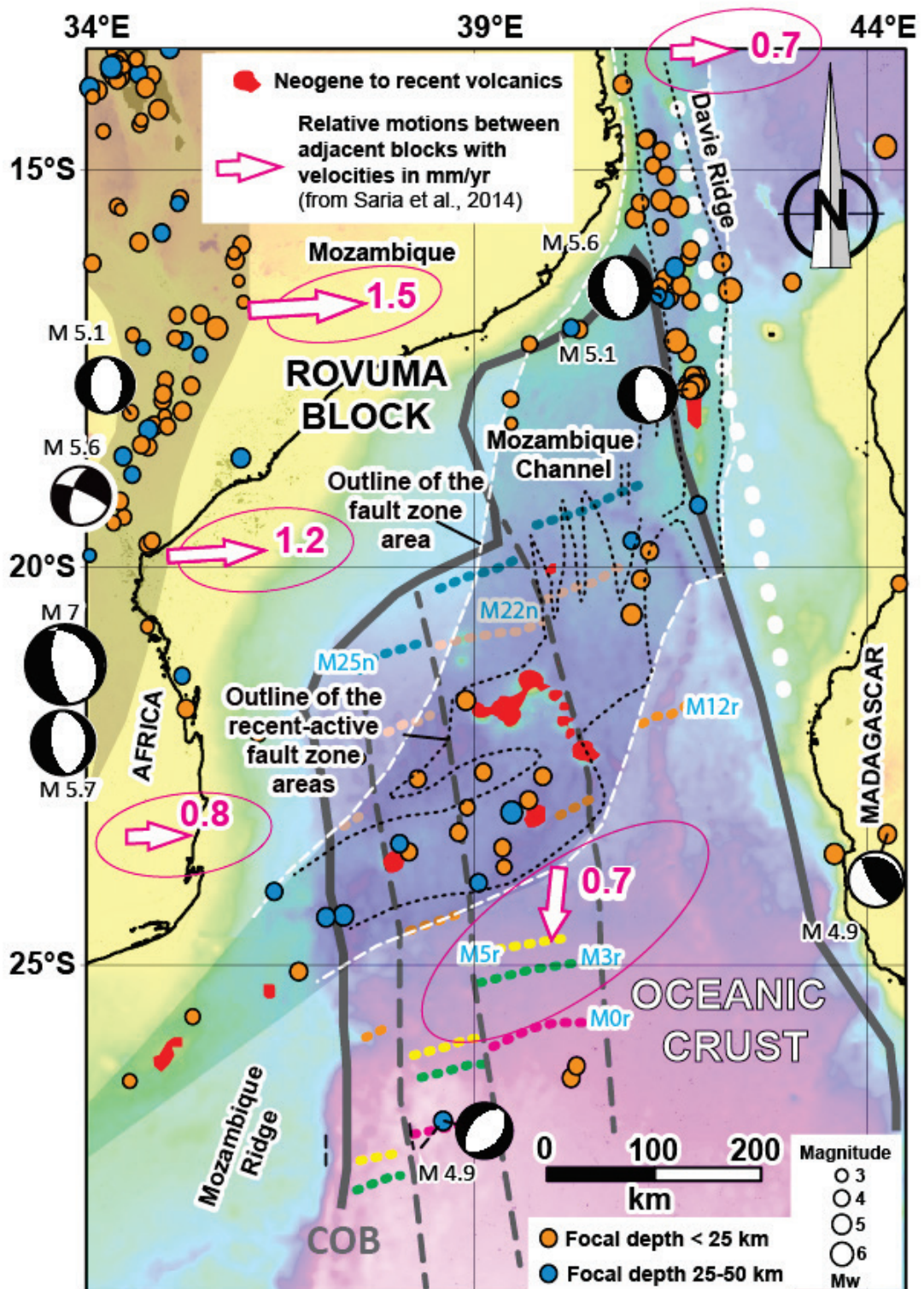
645 **Fig. 9.** Multibeam map crossing a depression along the fault zone showing en-échelons border
646 fault system characterizing a normal-dextral movement.

647

648

649

650



651

652

653

654 **Fig. 10.** Structural sketch-map of the Mozambique channel area (see location in Fig. 1)
655 showing the extent of the fault zone crossing the Mozambique Channel from NE to SW with
656 the location of the main corridors of recent to active faults (area bounded by white dotted
657 lines: fault zone studied in this paper; area bounded by black dotted lines: active fault zones).
658 grey areas correspond to the western and eastern branch of the EARS and the fault system
659 area described in this paper. Thick dotted line: Davie Ridge. Earthquake depths from the
660 NEIC catalog (USGS). Earthquake focal mechanisms from the Global Centroid Moment
661 Tensor database (Ekström et al., 2012). Pink arrows: relative motions between plate tectonic
662 blocks from Saria et al. (2014). Elevation/bathymetry grid from GEBCO. In red: main
663 volcanic systems. Location of the oceanic crust and oceanic fracture zones compiled from
664 Konig and Jokat (2010), Leinweber and Jokat (2012), Davis et al. (2016) and Mueller and
665 Jokat, (2017). Magnetic anomalies are from Davis et al. (2016). COB: Continent-Ocean
666 Boundary.

667

668

669 **Supplementary files**

670

671

DATE	TIME	LON	LAT	DEPTH	AUTHOR	MW	STRIKE	DIP	RAKE
24/07/1991	54:52.4	34.62	-18.3	24.7	HRVD	5.1	0	45	-90
22/02/2006	19:07.8	33.33	-21.2	12	HRVD	7	172	65	-78
23/02/2006	23:42.2	33.18	-21.33	12	HRVD	5.7	172	58	-91
17/09/2006	24:54.5	41.71	-17.54	19.6	GCMT	5.1	174	52	-86
24/09/2006	56:21.7	41.78	-17.59	12	GCMT	5.6	171	50	-89
09/10/2011	47:16.8	38.88	-26.89	30.8	GCMT	4.9	44	40	-86
25/01/2013	37:02.1	43.58	-23.73	24	GCMT	4.9	149	70	102
24/06/2017	02:37:20	34.48	-19.42	27	GCMT	5.6	292	67	163

672 **Table S1** – Earthquake focal mechanisms used in this paper.

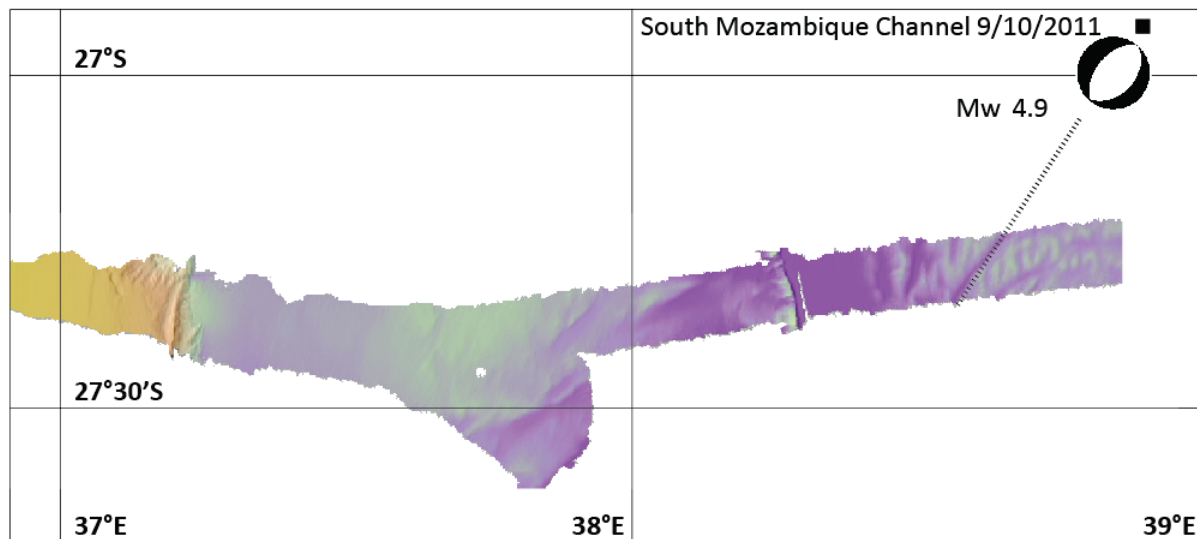
673

674

675

676

677

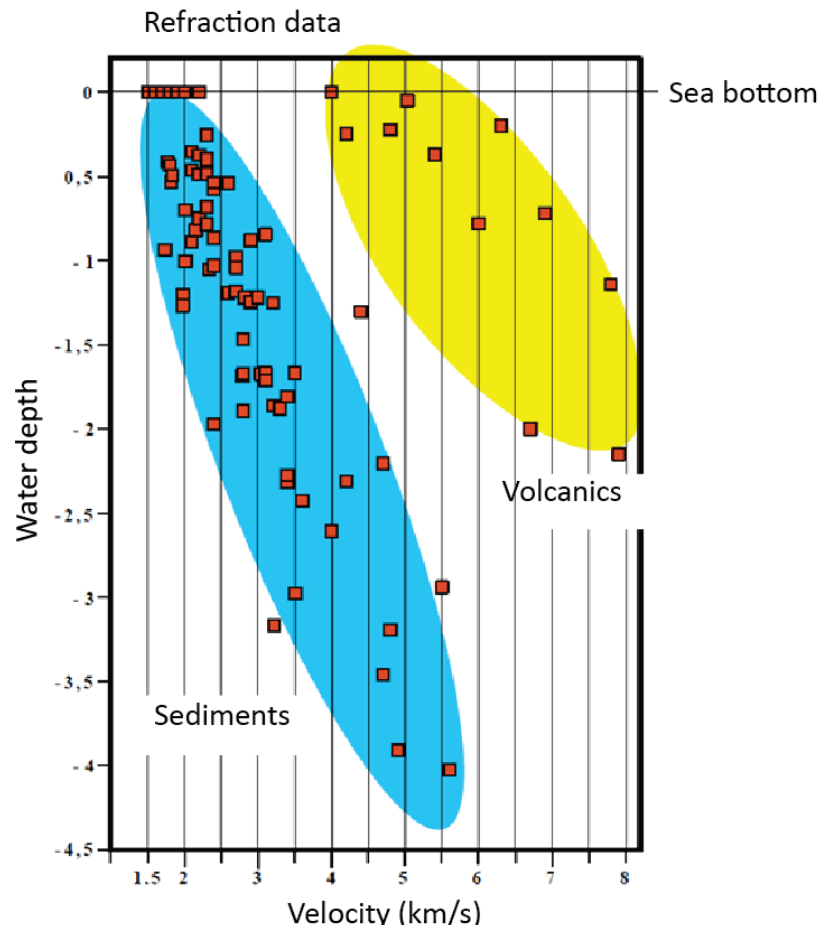


678

679

680 **Fig. S1** – Available bathymetric data close to the Mw 4.9 earthquake (9/10/2011) south of the
681 Mozambique Channel.

682

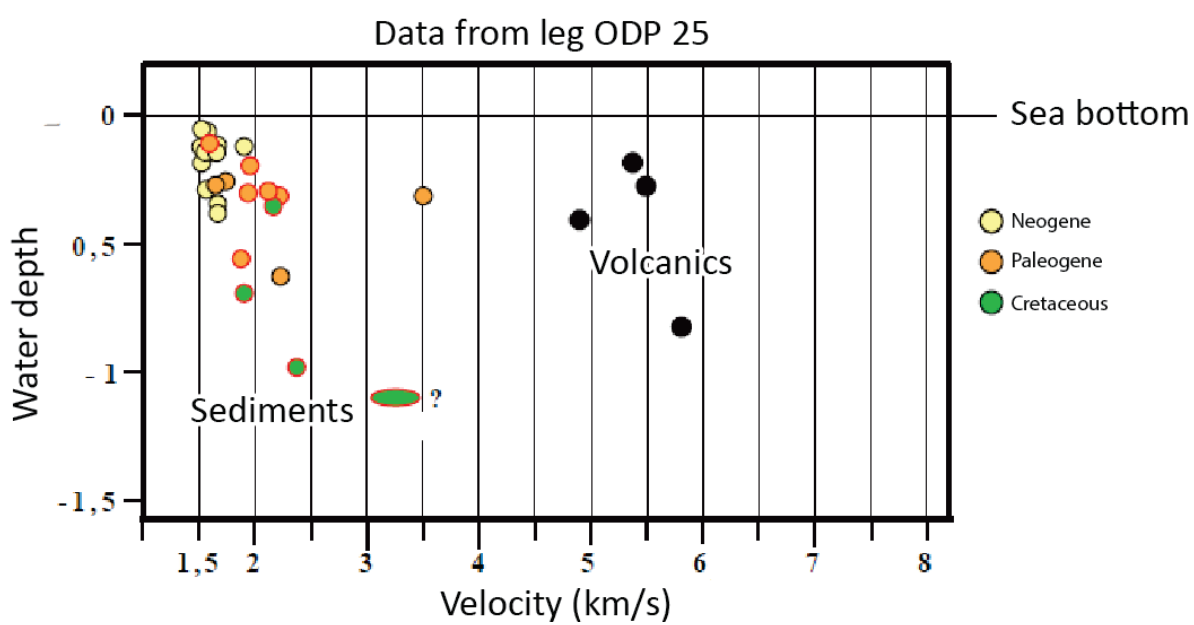


683

684

685 Fig. S2 – Seismic velocities deduced from refraction studies (from unpublished IFP rapport).

686



687

688

689 **Fig. S3** – Seismic velocities deduced from available well data (ODP leg 25, wells 242, 248, 250).

690